Annals of Warsaw University of Life Sciences - SGGW
Forestry and Wood Technology № 83, 2013: 185-190
(Ann. WULS - SGGW, For. and Wood Technol. 83, 2013)

Structure-property relationships – a study on the growth ring scale of Norway spruce

CHRISTIAN LANVERMANN[1)], SERGIO SANABRIA[1)], FALK WITTEL[1)],
PETER NIEMZ [1)], UWE SCHMITT [2)]
[1)]Institute for Building Materials, ETH Zurich, Switzerland
[2)]Thünen Institute of Wood Research, Hamburg, Germany

Abstract: *Structure-property relationships – A study on the growth ring scale of Norway spruce.* The growth ring structure of softwoods with its alternating earlywood and latewood bands is well-known. In this study, the structure-property relationships within growth rings of Norway spruce (*Picea abies* (L.) Karst.) are investigated. The use of SilviScan® and electron microscopy shows the great intra-ring variability of density and microfibril angle as well as cross-sectional cell dimensions. This variability is reflected in the full-field moisture-induced deformation within the hygroscopic range as determined by digital image correlation. Whereas radial swelling closely follows the density distribution within the growth ring with the highest deformation in the dense latewood, the corresponding tangential deformation is constant throughout a growth ring in the boundary-unaffected region of the sample. The application of a simple FEM model and the selective activation of the different tissues shows that radial swelling basically is dominated by earlywood, whereas tangential swelling is a complex interaction of expansion and contraction and needs the contribution of all tissues to fully develop. This behavior is reflected in the swelling of macroscopic samples with varying growth-ring widths and therefore varying portions of early- and latewood. In order to analyze local moisture concentration, neutron imaging (NI) and digital image correlation (DIC) were combined. This combination enables the calculation of volumetric as well as gravimetric moisture content. Whereas the former closely follows density distribution with the highest volumetric concentrations in latewood, the latter basically is constant throughout the growth ring.

Keywords: anisotropy, Norway spruce, growth rings, swelling, moisture content, structure, MOE, UTS, full-field, FEM, neutron imaging,

INTRODUCTION

The highly anisotropic behavior of bulk wood with respect to its principle directions (radial (R), tangential (T), and longitudinal (L)) is well known. This anisotropic behavior is not only found on the macroscopic scale but also on the cell wall level (Nakato 1958) and for the different tissues of earlywood (EW) and latewood (LW) (Derome et al. 2011; Rafsanjani et al. 2013). Where on the cell wall level, the anisotropic behavior with respect to cell wall orientation (parallel or perpendicular) is a consequence of its layered structure, the anisotropic behavior of EW and LW is mainly based on the transverse cell geometry as introduced by Gibson and Ashby (1988) for honeycombs. Furthermore, Rafsanjani et al. (2012a) studied the influence of geometrical disorder on the anisotropic behavior of EW and LW and the moisture-induced deformation behavior of single growth rings using environmental scanning microscopy and computational upscaling techniques (Rafsanjani et al. 2012b).

However, the behavior of single growth rings is not directly transferable to the situation in bigger samples where several growth rings and the interaction of the different tissues influence on the overall behavior.

This study is part of a greater project modeling wood under moisture loading on different hierarchical levels. Its aim is to experimentally determine the structure-property relationships on a growth-ring scale as part of bigger samples.

MATERIALS AND METHODS

In the following, the used material and the applied techniques are presented. Since the investigations involve various different experimental setups, they are only very briefly described.

Wood characterization

All experiments of the current investigation were conducted on samples from a single stem of Norway spruce (*Picea abies* (L.) Karst.) originating from Dielsdorf, Switzerland (approximately 450m above sea level). The characterization of this stem with regard to density, microfibril angle (MFA), transverse cell geometry and topochemical lignin content was accomplished using a SilviScan® apparatus, electron micrographs and microspectrophotometry, respectively (Lanvermann et al. 2013b).

Full-field swelling

The full-field swelling was determined contactless using a commercial digital image correlation package (Correlated Solutions, USA). This technique is based on the cross-correlation of similar gray value distributions, also known as digital speckle photography. Therefore, a fine random gray value pattern is applied on the surface of the sample. The individual deformation fields are acquired by cross-correlation with a reference image (in this case in an oven dry state). In order to gather quantitative data, image-processing techniques were applied to segment the full-field data into individual growth rings (see Lanvermann et al. 2013c). The samples were conditioned in adsorption up to 95% RH. Furthermore, a FEM model consisting of four consecutive growth rings was used to reveal the contribution of EW and LW on the overall swelling. Hereby, the consistent mechanical dataset of Perrson (2000) was used.

Local Moisture Content

In order to analyze the local moisture content, defined as the mass of water over the local dry density, within single growth rings of the stem, two techniques were applied: neutron imaging to measure the local amount of water and digital image correlation for deformation compensation as described above. For a detailed description of the applied technique see Lanvermann et al. (2013a). The samples were conditioned in a custom box and subjected to a complete ad- and desorption cycle.

Distribution of mechanical properties within growth rings

The distribution of the mechanical properties (modulus of elasticity (MOE), ultimate tensile strength (UTS)) within growth rings in tension was assessed on series of small dog-bone shaped specimens using a micro-tensile testing device (Deben, UK, 300N capacity). Therefore, samples containing one single growth ring were cut into thin slices (300 μm for EW and 150 μm for LW), punched into dog-bone shape and then tested while the strain was measured optically.

Swelling of macroscopic samples

In order to compare the results on a growth-ring level with the sorption and moisture-induced deformation of bulk wood (length scale: several cm), samples with dimensions of 60x60x25mm (RxTxL) were subjected to a complete ad- and desorption cycle at comparable RH steps as the ones in the experiments on the growth ring scale (see Fig. 2E). At equilibrium conditions, the samples weight was recorded as well as their dimensions.

RESULTS

The representative results for the structural and topochemical characterization of the tested material are given in Figure 1. Where the radial cell dimension (lumen + 2 cell walls) decreases from EW with about 50μm to LW with about 10μm, the tangential cell dimension only decreases by about 10μm. The trend, as observed in the corresponding cell wall thicknesses (data not shown), is reversed. This is clearly reflected in the density progression

with the low-density EW and the high-density LW. The mean MFA decreases from EW to LW from about 22° to about 10°. The absorbance, as a semi-quantitative measure for the lignin content only slightly increases from EW to LW. This can mainly be attributed to thicker middle lamellae in LW (Lanvermann et al. 2013b).

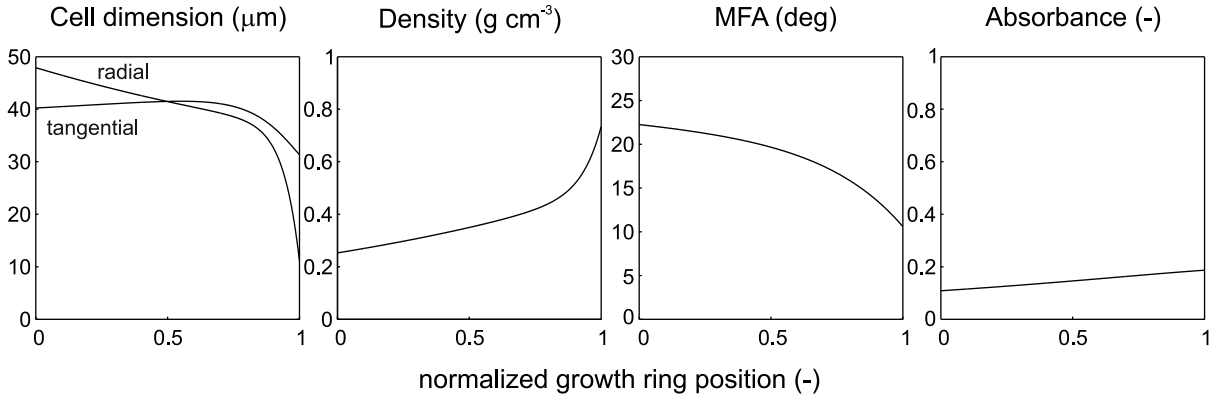

Fig. 1. Representative main structural parameters of the investigated stem (analytical fits). Please note that EW is denoted by 0 and LW by 1.

The main experimental results of this study are as follows: mechanical tests (Fig. 2A), swelling for individual growth rings (Fig. 2B), contribution of EW and LW on the local swelling using a FEM model (Fig. 2C), local gravimetric moisture content (Fig. 2D.1) and selected results from the swelling of macroscopic samples (Fig. 2D.2 – 2E).

It can clearly be seen that all tested mechanical properties, namely MOE in longitudinal (Fig. 2A.1) and tangential direction (Fig. 2A.2)as well as the ultimate tensile strength (Fig. 2A.3) follow the density trend with the highest values found in LW and the lowest values found for EW. The local swelling within growth rings in radial direction (Fig. 2B.1) also follows the density progression where the highest swelling strains for all tested relative humidities are found for LW and the lowest ones for EW. However, the tangential strain (Fig. 2B.2) is constant for the entire growth ring. This results in a swelling ratio (anisotropy) that is highest in EW and lowest (close to 1) in LW (Fig. 2B.3).

The results of a FEM model consisting of four consecutive growth rings show a good overall agreement with the experimental values (Fig. 2C). Furthermore, the selective activation of EW/TW and LW reveals that radial swelling (Fig. 2C.1 dash-dot line) is basically dominated by the swelling of EW (when LW does not swell) and tangential swelling is a complex interaction of tension and compression and needs the contribution of all tissues to fully develop. This impressive interaction can be seen for the case where only LW is allowed to swell (dashed line). LW expands in the tangential direction, is put under tension and this produces a Poisson effect that leads to a contraction (negative strain) of EW. This principle explains the constant tangential swelling as shown in Fig. 2B.2 where EW is forced to deform to the same extent as LW.

Despite the presented high gradients with respect to the mechanical properties and local swelling behavior, the local gravimetric moisture content is constant throughout the growth ring (Fig. 2D.1) which can be attributed to the constant chemical composition of EW and LW. The visible drop in EW is mainly based on measurement uncertainties in the region of the growth ring boundary which is prone to artifacts due to smoothing effects in the neutron images and especially in the local strain determination (Lanvermann et al. 2013a). Please note that, although the RH levels are comparable, the samples were not fully equilibrated due to experimental constraints.

The mean density of macroscopic samples is a measure for the mean growth-ring width of the sample (data not shown). This correlation between growth-ring width and density is already known for *Picea* spp. (Kollmann 1951). It is based on a constant LW thickness,

whereby only EW thickness varies with growth ring width. The constant moisture content as shown for the growth ring level can be extended to macroscopic samples as indicated in Fig. 2D.2 within the observed density and humidity range.

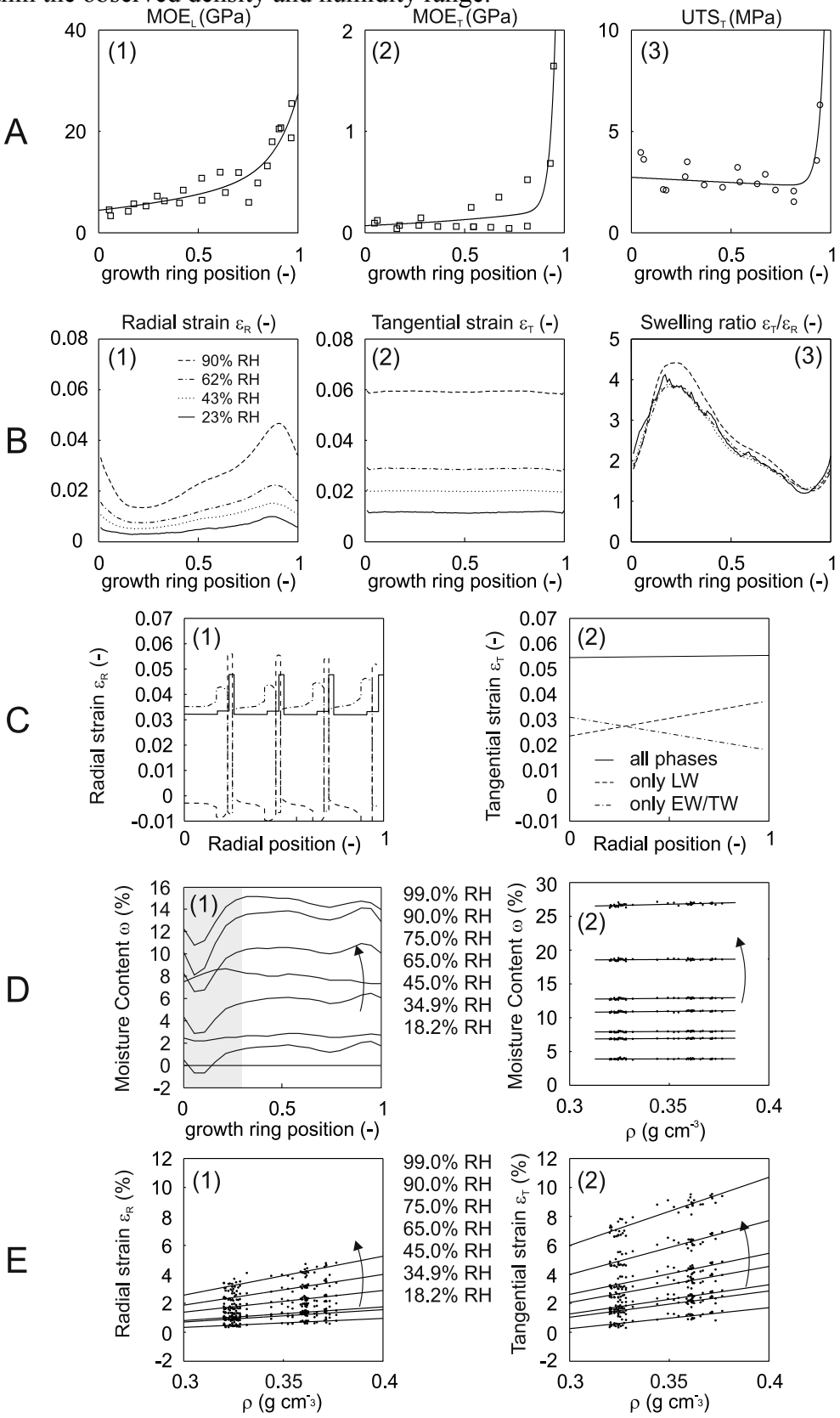

Fig. 2. Main experimental results of the study: (A) mechanical properties, (B) local swelling, (C) FEM results on the contribution of EW and LW, (D.1) local MC, and tests on macroscopic samles (D.2- E)

The correlation of the transverse swelling strains (radial and tangential) with the samples' dry density is given in Fig. 2E. A positive correlation is found for both directions where an increase in density leads to an increased swelling strain for all humidity levels. The increased swelling is mainly based on the higher LW percentage with increasing density. The slope of this linear relation is found to increase with increasing humidity for both directions which can be seen from the higher differential swelling as implicitly shown in Fig. 2B.1. Furthermore, with increasing density the transverse anisotropy decreases.

In general, mechanical properties and moisture-induced deformations are highly influenced by the layered growth-ring structure, whereas the sorption properties in equilibrium conditions are not influenced. The trends as observed on macroscopic samples can be well explained by the varying content of EW and LW.

REFERENCES

1. DEROME D., GRIFFA M., KOEBEL M., CARMELIET J. 2011: Hysteretic swelling of wood at cellular scale probed by phase-contrast X-ray tomography. *Journal of Structural Biology*, 173(1), 180-190.
2. GIBSON L. J., ASHBY M. F. 1988: *Cellular Solids - Structure and Properties*, Pergamon Press, Oxford.
3. KOLLMANN F. 1951: *Technologie des Holzes und der Holzwerkstoffe - Erster Band: Anatomie und Pathologie, Chemie, Physik, Elastizität und Festigkeit*, Springer Verlag, Berlin.
4. LANVERMANN C., SANABRIA S. S., MANNES D., NIEMZ P. 2013a: Combination of Neutron Imaging and Digital Image Correlation to Determine Intra-Ring Moisture Variation in Norway Spruce. *Holzforschung*.
5. LANVERMANN C., SCHMITT U., EVANS R., HERING S., NIEMZ P. 2013b: Distribution of structure and lignin within growth rings of Norway spruce. *in print in Wood Science and Technology*.
6. LANVERMANN C., WITTEL F. K., NIEMZ P. 2013c: Full-field moisture induced deformation in Norway spruce: Intra-ring variation of transverse swelling. *Submitted to European Journal of Wood and Wood Products*.
7. NAKATO K. 1958: On the cause of the anisotropic shrinkage and swelling of wood. IX. On the relationship between the microscopic structure and the anisotropic shrinkage in the transverse section. *J. Jpn. Wood. Res. Soc.*, 4(4), 131-141.
8. PERSSON K. 2000: Micromechanical modelling of wood and fibre properties. Doctoral Thesis, Lund University.
9. RAFSANJANI A., DEROME D., CARMELIET J. 2012a: The role of geometrical disorder on swelling anisotropy of cellular solids. *Mechanics of Materials*, 55(0), 49-59.
10. RAFSANJANI A., DEROME D., WITTEL F. K., CARMELIET J. 2012b: Computational up-scaling of anisotropic swelling and mechanical behavior of hierarchical cellular materials. *Composites Science and Technology*, 72(6), 744-751.
11. RAFSANJANI A., LANVERMANN C., NIEMZ P., CARMELIET J., DEROME D. 2013: Multiscale analysis of free swelling of Norway spruce. *Composites Part A: Applied Science and Manufacturing*, 54(0), 70-78.

Streszczenie: *Zależność pomiędzy strukturą a właściwościami – badania nad przyrostem rocznym świerka*. Struktura przyrostu rocznego drzew iglastych z widocznymi warstwami drewna wczesnego i późniego jest dobrze znana. W prezentowanej pracy zbadano zależności struktury przyrostu rocznego od własności drewna świerka (*Picea abies* (L.) Karst.). Przy użyciu SilviScan® oraz mikroskopu elektronowego zbadano wariacje struktury przyrostu, kąt pochylenia mikrofibryl i przekroje komórek. Zmienność ta jest widoczna w deformacji spowodowanej spęcznieniem drewna w zakresie higroskopijnym. O ile spęcznienie promieniowe jest ściśle związane z rozkładem gęstości w przekroju przyrostu rocznego, o największej deformacji w drewnie późnym, to spęcznienie w kierunku stycznym jest stałe w obrębie przyrostu. Zastosowanie metody elementów skończonych i selektywnej analizy strefy drewna wczesnego i późnego wykazuje, że spęcznienie promieniowe jest praktycznie determinowane przez drewno wczesne, natomiast spęcznienie styczne jest skomplikowaną interakcją rozszerzania i kurczenia się i potrzebuje pełnego przyrostu rocznego. Znajduje to odzwierciedlenie w pęcznieniu próbek makroskopowych ze zmienną szerokością przyrostów rocznych i związaną z tym zmienną wielkością stref drewna późnego i wczesnego. W celu analizy wilgotności lokalnych użyto obrazowania neutronowego oraz cyfrowej korekcji obrazu, umożliwiających w tej konfiguracji dokonanie obliczeń wolumetrycznych i grawimetrycznych rozkładu wilgotności.

Corresponding author:

Christian Lanvermann
Schafmattstrasse 6,
8093 Zurich, Switzerland
email: lanvermannchr@ethz.ch